Factors Influencing the Distribution of Maximum Specific Absorption Rates in Far Field Human Exposure Scenarios

Ovidiu Bejenaru[1], Catalin Lazarescu[1], Marius Valerian Paulet[1], Alexandru Salceanu[1], Marius Vasile Ursachianu[1]

[1] 'Gheorghe Asachi' Technical University of Iasi, Romania, Faculty of Electrical Engineering

ABSTRACT

The biological and health effects of electromagnetic fields are a current concern. With the aim of evaluating these effects, it is essential to estimate the levels of human exposure to various types of electromagnetic sources within different environments. These assessments could be performed by determining the current density distributions inside organs or tissues, by modeling the different mechanisms of electromagnetic exposure or even by modelling the development of effects in living beings. Everything should be done while considering various exposure scenarios. In this paper, we have determined, through simulations employing CST Suite Studio software, the specific absorption rates (SARs) values for a human body, averaged from the values for different 10 grams of tissue in different areas of the body, in the case of its exposure to an electromagnetic field generated by a source placed in the far field domain, where the human body is located in an empty room inside a building. We have used our previously tested 3D human body model that has the geometry of an elliptical cylinder. The simulated SAR values have been also compared with the reference levels accepted by the International Commission on Non-Ionizing Radiation Protection and IEEE Standards for Safety Levels for both public and professional exposure.

Corresponding author: Alexandru Salceanu, e-mail: asalcean@tuiasi.ro

1. GENERAL FRAMEWORK

Aiming to protect humans against different electromagnetic field (EMF) sources, numerous countries around the world have already proposed and recommended various safety standards and regulations. The actual standards for human exposure entail, according to the selected frequency domain, totally different associated methods and measurements for defining the so-called basic restrictions, with either internal induced current density or internal electric field (up to 100 kHz), localised specific absorption rate (SAR; from 100 kHz up to 10 GHz) or power density (from 10 GHz to 300 GHz) establishing the corresponding safety limits.

The results presented in this article are mainly related to SAR modelling and simulations; therefore, we refer to the 10 MHz–10 GHz frequency range. In relation to this particular frequency range, if the distance between the EMF source and human subject is greater than 5 metres, this can be considered a 'far field' approach. The body is exposed not only to the direct (uniform)

plane wave but also to the reflected waves. In addition, it must be said that, although the incident wave is 'uniform', the way the energy is absorbed by the body is significantly non-uniform, due to both the different dielectric properties of the various tissues and organs and also the possible resonance phenomena that may occur.

Various international organisations are concerned with establishing measurable limits (considered non-dangerous) of exposure for both the general public and professional workers [1]-[7]. Additionally, in the military field, there are further specific regulations regarding limiting exposure to non-ionising electromagnetic radiation [8], [9].

Regarding the radio-frequency spectrum (and above), an important limit for the incident power density is 1.0 mW/cm² [3]. This value should guarantee that, in any part of the exposed body, the basic restriction on the local SAR (2 W / kg averaged over any 10 g of tissue in the head and trunk regions and 4 W / kg for the limbs) is never exceeded [1], [3].

As computer processing speeds and techniques continue to significantly improve, SAR determinations using numerical methods for different types of exposure can even be performed for realistic models of the human bodies.

The human body can be 3D modelled with a geometry more or less detailed depending on the number of voxels and the electrical characteristics of the organs and tissues. Some of the first basic models of the human body for the numerical simulation of power absorption were the rotational cylinder [10] for frequencies below 600 MHz, the prolate spheroid [11] for frequencies above 10 GHz and the multi-layered cylinder [12] for frequencies between these. There are significant differences between these simplified 3D models with uncomplicated geometries and quasi-complete (realistic) voxel models of the human body developed over many years by very powerful software companies (a well-known example being the Hugo model [13]). One consideration of these 3D models is that they must allow scaling according to the very wide variety of human physical dimensions [14]. Therefore, the number of voxels needed for a specific model could be extremely high, and 'slice by slice' processing of various images could involve a considerable amount of time and resources. A solution to this issue could be the use of simplified 3D models in such cases.

Different 3D electromagnetic simulation software programs offer very accurate and efficient computational solutions for electromagnetic design and analysis. Electromagnetic simulation software allows engineers to efficiently investigate the electromagnetic properties of (sub)systems, computing the field distribution at specific points or zones of interest [15]-[17].

2. BACKGROUND OF OUR APPROACH

For real human being, the SAR values will generally vary from those calculated using numerical methods applied to different simpler models (sphere, cylinder and rotational ellipsoid) of the human body. Obviously, to accurately calculate the average SAR at high frequencies, much more realistic models of the human body are strongly required.

Nevertheless, as an entry point to the study of any type of human exposure to non-radiating EMFs, a simplified intermediary model could be accepted, as it would offer positive outcomes that could be considered in further approaches and developments.

Using numerical simulations provided by the CST Studio Suite software, we have determined the SAR at the surface of the proposed 3D human body model. The EMF source was located outside the building, while the subject is inside an empty room with concrete walls located on the ground floor. The distance between the source and subject is higher than 5m; consequently, the incident wave is plane (for the whole spectrum of interest) and the set-up should be considered 'far field'.

The simplified 3D model proposed and used in this study is considered to be a nude one (without clothes). It has been proven that the average SAR is affected by the thickness of any worn clothes. Some researchers have previously investigated this effect [5] using the multi-layered cylindrical model while also considering the introduced power loss [18].

3. MATERIAL AND METHODS

Specific absorption rate is generally used to quantify the electromagnetic energy absorbed by the human body from different types of electromagnetic sources. Different numerical methods are used for SAR computations, but the most

prominent numerical methods employed are Finite-difference time-domain (FDTD) and Finite integration technique (FIT), [19], [20]. These methods consider the volume of study (the actual human model and the neighbouring space) as being composed of a very large number of cells identified by indexes (i, j, k), with the field components being defined at fixed locations. Maxwell's equations in the time domain are then discretised by using the finite-difference approximations for time and space derivatives.

The time-stepping system resulting from the discretisation of the Maxwell's equations is solved by imposing the excitation field as a function of time with adequate initial and boundary conditions. For initial conditions, all the components of the electromagnetic field are equal to zero at the initial starting time step.

In this paper, the incident electric field has been supposed to have the characteristics of a plane wave with time-harmonic behaviour (far field hypothesis). Under these assumptions, the local SAR at each cell is given by the equation (1):

$$SAR(i, j, k) = \sigma(i, j, k)\big[E_x^2(i, j, k) + E_y^2(i, j, k) + E_z^2(i, j, k)\big]/\rho(i, j, k) \tag{1}$$

where $\sigma(i, j, k)$ and $\rho(i, j, k)$ are the space dependent conductivity and density, respectively, of the (i,j,k) voxel. In equation (1), the peak value of the electric field components has been considered.

The skin tissue of the human body (mainly due to 'skin' effect but also due to its conductive properties) plays the role of 'electromagnetic shield' in protecting the inner organs against microwave exposure. This is the main reason for the fact that the human body model here proposed is covered with 'skin material' from the CST library. For instance, at 900 MHz, for skin, relative permittivity is 0.86, conductivity is 0.86 S/m and density is 1100 kg/m³, with no magnetic properties.

The way SAR varies depending on the electrical properties of the skin at different frequencies can be analysed using numerical methods, and the skin properties (as tissue) can be estimated at an analytical level using the Debye equation.

We have also considered the relative complex permittivity $\dot{\varepsilon}_r$ of the skin (according to Debye dispersion characteristics) with two relaxation time constants, τ_1 and τ_2 [21]. The dispersion equation is as follows:

$$\dot{\varepsilon}_r = \varepsilon_r - j\frac{\sigma}{\omega\varepsilon_0} = \varepsilon_\infty + \frac{\varepsilon_{S1} - \varepsilon_\infty}{1 + j\omega\tau_1} + \frac{\varepsilon_{S2} - \varepsilon_\infty}{1 + j\omega\tau_2}, \tag{2}$$

where ε_r is the relative permittivity and σ is the conductivity. Here ε_∞ is the relative permittivity at the highest frequency, while $\varepsilon_{S1} + \varepsilon_{S2} - \varepsilon_\infty$ is the relative permittivity for DC. If these parameters can be estimated by matching the measured data for several specific frequencies, the electrical properties of skin tissue for these frequencies might be deduced.

In our study, we have determined the SAR values for 10 g of specific tissue, in the following referred to as "SAR Max (10 g)". Spatial mediation is applied, the highest value being retained. We have used a quasi-simplified homogeneous 3D model of the human body and a 900 MHz source (a representative frequency for the Global System for Mobile communications, GSM).

The 3D model of the human body designed and used in this study is an updated version of a simplified 3D model previously used in [22]-[24]. For the design of the 3D human body model, we have used the CAD interface from the 'Modeling' section of the CST software. The developed 3D model has been 'built' from circular rotational bodies with the exception of the trunk part,
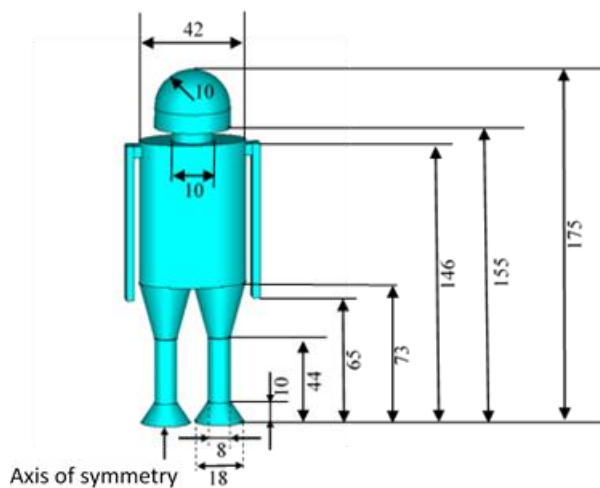
Figure 1. Proposed 3D model of a human body. All dimensions are expressed in centimetres (cm).

which uses an elliptic cylinder (see Figure 1). This body shape design is much closer to reality than the variant used in other studies with a circular cross section, and it allows for different evaluations of field distribution and induced currents on the surface of the model. We have made these minor modifications to the shape and dimensions of the human body cross-sections to provide a more realistic approach. As can be seen, the height of our model is 175 cm, which is average for a male person in standing position.

The computation background has been provided by 'Microwave Studio' module from the CST Studio Suite software. The far-field source is considered to be a linear polarised uniform plane wave with the incident electric field of E_{zinc} parallel with the Oz axis, as presented in Figure 2.

The plane wave irradiates parallel to the model from the minus direction of the y axis. The value of the incident electric field is considered to be 41.25 V/m for the general public exposure assessment and 90 V/m for the professional exposure simulation. These two distinctive values have been chosen in accordance with the acceptable limits for public and professional exposure established by the International Commission on Non-Ionizing Radiation Protection (ICNIRP).

In accordance with our research interests, to determine the SAR Max (10 g) distribution on the surface layer of our 3D model, we have used the previously mentioned specific characteristics of human skin at 900 MHz.
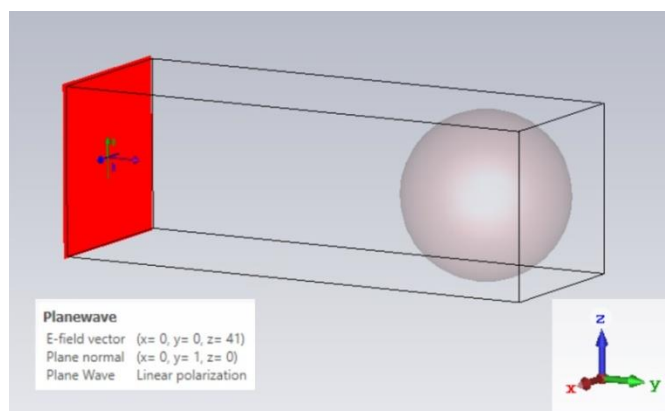

Figure 2. Direction of the incident plane wave toward the object under testing.

Different exposure scenarios have been considered. SAR values have been obtained for five simulations with the following distinct conditions:

Case A: the human body is directly positioned on the ground without (insulated) shoes on his feet (no shielding, no ground isolation; see Figure 3.a);

Case B: there is a concrete floor (no shielding, partially isolated from the ground; see Figure 3.b);

Case C: the human body is placed inside an airtight concrete room (good shielding; see Figure 3.c);

Case D: the human body is inside the same room but with one closed window (shielding and partially shielded aperture; see Figure 3.d);

Case E: the human body is inside the same room but with one open window (shielding with aperture; see Figure 3.e).

In all of the scenarios presented above, the 3D model of the human body is placed in the middle of the room in an unchanged position.

The ground (soil) has also been modelled in the CAD section of the CST Studio Suite software. Its rectangular shape has been designed as a parallelepiped with dimensions $800 \times 800 \times 30$ cm³ in Ox, Oy, Oz directions. The soil material used was the 'Loamy' type (dry) from the CST library materials. The walls, floor and ceiling of the room are simulated as being made from concrete with a minimum age of one year old; this material can also be found in the CST library. The room is a parallelepiped with dimensions $500 \times 200 \times 200$ cm³ in Ox, Oy and Oz directions, respectively.

Additionally, we have chosen the 'lead glass' window material from the CST library, as we were interested by the study of its refractive behaviour [25].

a) Case A   b) Case B

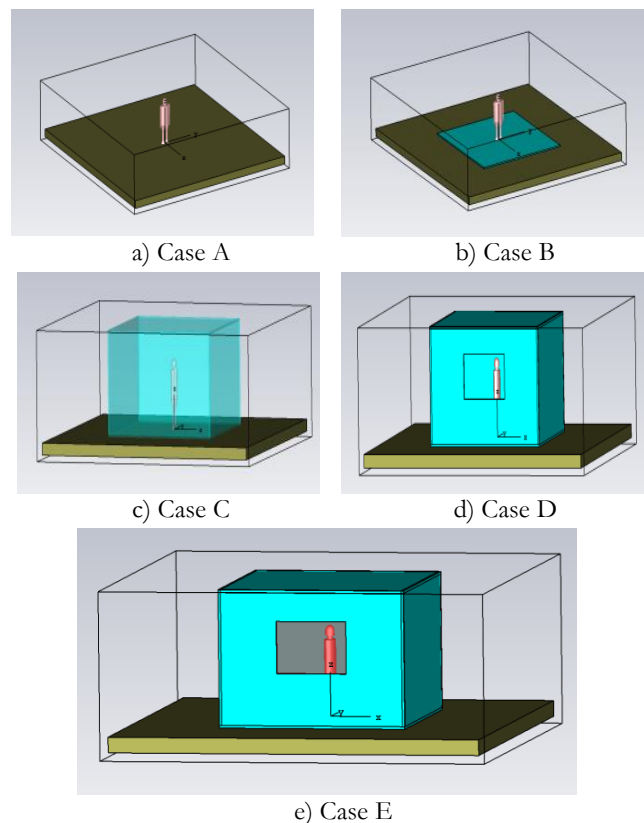c) Case C   d) Case D

e) Case E

Figure 3. Different simulation scenarios for determining the SAR Max (10 g) distribution on the surface of our model.

Furthermore, in the CST software, under the 'Simulation' menu for background properties, the material type was set as 'normal' and the space as 'air-filled', air (or free space) having well-known electromagnetic properties. For the surrounding space, we have set a value of 15 cm for the Lower X, Upper X, Lower Y, Upper Y, Lower Z, Upper Z distances, applied in all directions. These distances extend the virtual surrounding box of our model. By default, the CST software considers the space surrounding a structure as being $\lambda/8$ cm in all directions. Other approaches assume this space to be a quarter of a wavelength in each direction around the structure. We have extended the space around the structure in each direction with a length approximately equal to $\lambda/2$ (for a 900 MHz frequency, this means about 15 cm).

The 'boundary' was set as 'open', with extra space in all directions. The frequency range (more precisely, F_{min} and F_{max}) was set according to the frequencies of interest. Unjustified augmentation of the frequency domain can lead to a higher number of mesh cells, which would increase the simulation time accordingly. The frequency range has been set to 0 - 1.5 GHz in the Simulation menu.

Before starting the simulation process to determine the SAR Max (10 g) values, the 'Time Domain Solver' should be selected. To avoid a situation where the steady state energy criterion is not satisfied, we extended the maximum number of pulses from 20 to 50. This is because, for complex cases during the simulation process, using the Time Domain Solver, the program cannot successfully complete the simulation process. When a larger maximum pulse number is used, the solver works properly, and the results display with acceptable errors. This is an 'adaptive meshing type' solution, which aims to save time and hardware resources. The mesh type is considered to be hexahedral, and the source type selected is 'Plane Wave'. We can control the mesh density for our structure by increasing the number of lines per wavelength.

The simulations were carried out with the default value of 10 lines per wavelength, while lower mesh limit was set by default
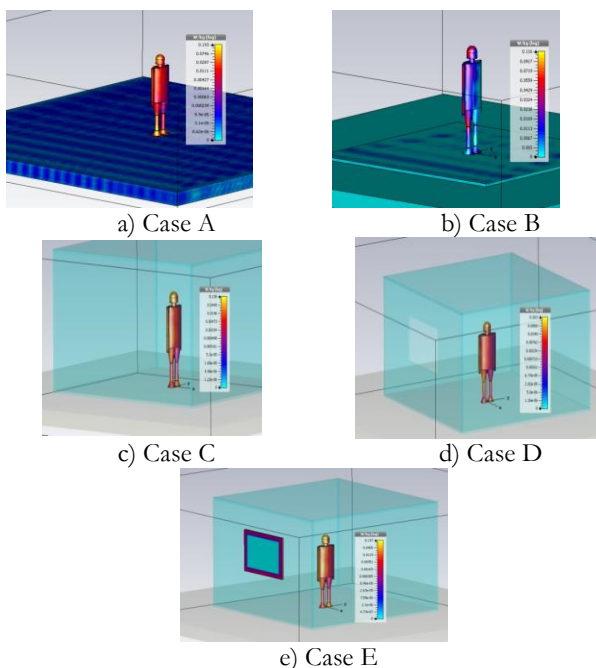
Table 1. SAR Max (10 g) values on different areas of the surface of the 3D model of the human body (10 lines per wavelength, external electric field E_{zinc} = 41.25 V/m [public exposure limit] and 900 MHz frequency).

Location	SAR Max (10 g) in W/kg				
	Case A	Case B	Case C	Case D	Case E
Head	$8.31 \cdot 10^{-2}$	$7.01 \cdot 10^{-2}$	$4.33 \cdot 10^{-2}$	$6.04 \cdot 10^{-2}$	$5.17 \cdot 10^{-2}$
Trunk	$2.17 \cdot 10^{-2}$	$2.45 \cdot 10^{-2}$	$1.07 \cdot 10^{-2}$	$1.87 \cdot 10^{-2}$	$1.33 \cdot 10^{-2}$
Limbs	$1.71 \cdot 10^{-1}$	$6.45 \cdot 10^{-2}$	$4.80 \cdot 10^{-2}$	$5.59 \cdot 10^{-2}$	$4.73 \cdot 10^{-2}$

Table 2. SAR Max (10 g) values on different areas of the surface of the 3D model of the human body (10 lines per wavelength, external electric field E_{zinc} = 90 V/m [professional exposure limit] and 900 MHz frequency).

Location	SAR Max (10 g) in W/kg				
	Case A	Case B	Case C	Case D	Case E
Head	$3.91 \cdot 10^{-1}$	$3.31 \cdot 10^{-1}$	$2.03 \cdot 10^{-1}$	$2.84 \cdot 10^{-1}$	$2.33 \cdot 10^{-1}$
Trunk	$1.17 \cdot 10^{-1}$	$1.21 \cdot 10^{-1}$	$5.78 \cdot 10^{-2}$	$8.93 \cdot 10^{-2}$	$6.29 \cdot 10^{-2}$
Limbs	$5.37 \cdot 10^{-1}$	$3.27 \cdot 10^{-1}$	$2.31 \cdot 10^{-1}$	$2.26 \cdot 10^{-1}$	$2.07 \cdot 10^{-1}$

to 7. These settings offer a good compromise to start with. Considering the fact that a complete convergence study (where the number of lines per wavelength was increased from 10 to 40 for a better mesh structure) has been previously carried out in a recent study [26], in the present work, we will take into consideration the conclusions drawn regarding the accuracy of the final values of SAR Max (10 g) obtained in these previous simulations.

4. RESULTS AND DISCUSSIONS

A simulation process for the determination of the distribution of SAR Max (10 g) values on the surface of a 3D model of the human body has been performed for different scenarios (Cases A–E, as previously defined).

Figure 4 presents these distributions. In all cases, we have set the mesh grid as 10 lines per wavelength. The external incident field has been set as 41.25 V/m (the upper accepted limit for exposure for the general public).

Table 1 summarises how exactly the SAR MAX (10 g) values vary for different regions of human body surface for the various cases (A–E).

Table 2 provides the same data for when the incident electric field is 90 V/m, i.e. the corresponding maximum value for occupational exposure. The cursor tool option from the CST software interface was fixed as 'Field' with the intention of searching the maximum values for SARs per 10 grams of (skin) tissue on the surface of our model.

a) Case A

b) Case B

c) Case C

d) Case D

e) Case E

Figure 4. SAR Max (10 g) distribution on the surface of 3D model of the human body due to an external electric field E_{zinc} = 41.25 V/m with 900 MHz frequency.
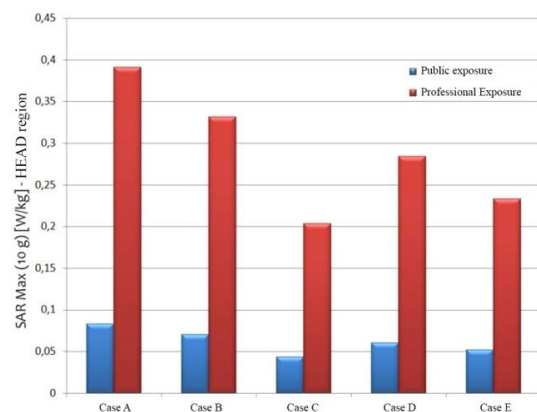

Figure 5. Comparative SAR Max (10 g) values for public versus professional exposure: head region.

Figure 6. Comparative SAR Max (10 g) values for public versus professional exposure: trunk region.
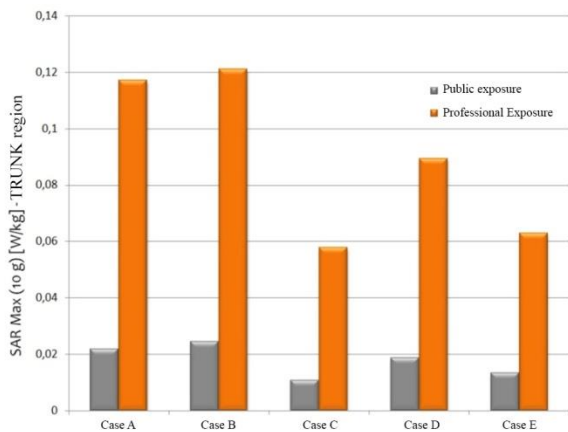

Figure 7. Comparative SAR Max (10 g) values for public versus professional exposure: limbs region.

Extracted from these tables, more intuitive SAR Max (10 g) values comparing public and professional exposure are illustrated in Figure 5 for the head area, Figure 6 for the trunk and Figure 7 for the limbs area.

From this comparative analysis (general public versus professional) of the SAR Max (10 g) values recorded for significantly different areas of the surface of the proposed model, it can be seen that the values for professional exposure are 3.2 to 5.4 times higher.

As expected, for the head and trunk areas, the SAR highest values have been recorded in Case A (open space, grounded) and the smallest values have been recorded in Case C (airtight, concrete walls). Somewhat surprisingly, for all three regions here studied (head, trunk, limbs), the exposure in the case of the open window is lower than in the case of the closed window (Case E versus Case D), even though it is assumed that 'lead glass' might have reflective properties. We suppose that a plausible explanation could be offered by the existence of the 'aperture effect' and some cumulative reflections.

It should be noted significant variation of SAR values exists between the two main types of scenario, i.e. scenarios with an open-air body (Cases A and B) versus scenarios with a body inside a building whose walls have shielding properties, e.g. reinforced concrete (Cases C–E).

Greater accuracy for the final SAR Max (10 g) values could be obtained by increasing the number of lines per wavelength in the mesh section of the CST software: in other words, using a finer mesh grid. Taking into consideration the previous studies performed by authors on this topic [26], [27], [28], it can be concluded that the mesh grid influences the simulated SAR values. More specifically, there is a 50 % increase in the simulated SAR values when 30 lines per wavelength are used in place of 10 lines per wavelength.

Due to the positioning of the human model inside the enclosure, we can also assume the presence of the multiple reflection phenomenon due to the reflectivity of the walls; this phenomenon might have had an impact on the final SAR values of the simulations.

5. CONCLUSIONS

We conducted a study assisted by CST software that aimed to simulate the average SAR values for 10 g of tissue on different areas on the surface of a 3D model of a human body (developed by the authors).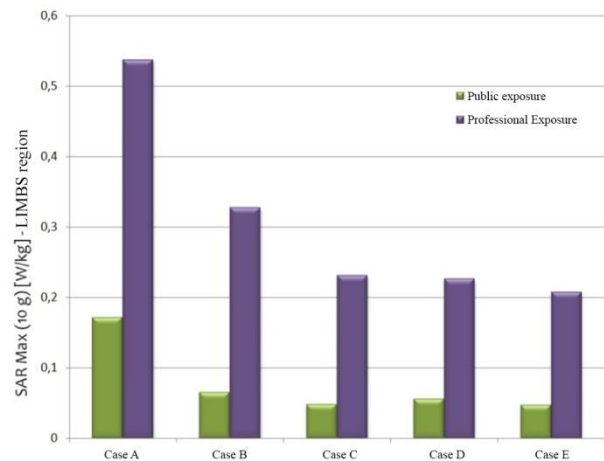 In the simulations performed, the human body model was located in the 'far field' region (the distance between source and 'victim' is longer than $\lambda/(2\,\pi)$). The incident value of the external electric field E_{zinc} (along the Oz axis) was specified as 41.25 V/m for simulations of general public exposure and 90 V/m for simulations of professional, controlled exposure. A frequency of 900 MHz was chosen, as it is the GSM mobile communication band. These values for the incident electric field have been selected as they are the maximum values admissible according to ICNIRP regulations. Therefore, the present study could have relevance to different exposure scenarios.

Using a 3D elliptical cylindrical geometry for the human body, electromagnetic simulations have been performed using the Microwave module of the CST Studio Suite software (published by Simulia).

Our study has been carried out taking into account the two main possible scenarios of a human body in relation to a transmitting antenna, i.e. being in open space or being inside a room with walls that have shielding/attenuating properties. The effect produced by the presence of a window in these scenarios, open or not (with glass also having protective properties), has been also studied.

The study was differentiated (even from the perspective of exposure risk) for the three main parts of the human body: head, trunk, and limbs.

Regarding the convergence of the SAR Max (10 g) values, this should be analysed in more details in a future study on effect of different positionings of the proposed model inside the enclosure.

We have concluded that the SAR Max (10 g) values obtained in our simulations using the CST software for this type of far field exposure are considerably lower than the acceptable ICNIRP values, which is in decent agreement with IEEE and EU standards for both types of exposure: residential and occupational.

REFERENCES

[1]   A. Ahlbom, U. Bergqvist, J. H. Bernhardt, J. P. Cesarini, L. A. Court, M. Grandolfo, M. Hietanen, A. F. McKinlay, M. H. Repacholi, D. H. Sliney, J. A J Stolwijk, M. L. Swicord, L. D. Szabo, M. Taki, T. S. Tenforde, H. P. Jammet, R. Matthes, International Commission on Non-Ionizing Radiation Protection, Guidelines for Limiting Exposure to Time-Varying Electric,

Magnetic, and Electromagnetic Fields (up to 300 GHz), Health Physics 74 (1998) pp.494-521.

[2] IEEE Standard for Safety Levels with Respect to Human Exposure to Radio Frequency Electromagnetic Fields, 3 kHz to 300 GHz, C95.i2005, Institute of Electrical and Electronics Engineers, New York, 2005.

[3] European Committee for Electrotechnical Standardization (CENELEC) Prestandards ENV 50166-2, Human exposure to electromagnetic fields. High frequency (10 kHz to 300 GHz), CENELEC, Brussels, Belgium, 1995.

[4] D. C. Dabala, D. Surcel, C. Szanto, Health Risk Assessment In Occupational EMF Exposure, 2nd International Symposium on Applied Sciences in Biomedical and Communication Technologies, Bratislava, Slovakia, 24-27 November 2009. DOI: https://doi.org/10.1109/ISABEL.2009.5373607

[5] S. Miclaus, P. Bechet, Near Field Radiofrequency Metrology and Occupational Exposure Assessment: In Situ Measurement and Accuracy Analysis, Proc. of the 20th International Conference on Applied Electromagnetics and Communications (ICECOM), Dubrovnik, Croatia, 20-23 September 2010.

[6] A. Paljanos, S. Miclaus, C. Munteanu, Near-field level emitted by professional radio communication devices: preliminary measurements and simulations for on occupational exposure assessment approach, Proc. of the 2014 International Conference and Exposition On Electrical Compatibility and Engineering in Medicine and Biology, Iasi, Romania, 2014, pp. 508-513.

[7] Directive 2004/40/EC of the European Parliament and of the Council, 29 April 2004, on the minimum health and safety requirements regarding the exposure of workers to the risks arising from physical agents (electromagnetic fields) (18th individual Directive within the meaning of Article 16(1) of Directive 89/391/EEC)

[8] S. Miclaus, P. Bechet, Occupational Exposure to Electromagnetic Fields Assessment of Personnel Serving Military Mobile Radio Communication Stations: A preliminary Study, Conf. Proc. of the 15th International Conference 'The knowledge based organization' (vol. 6), Land Forces Academy Publishing House, Sibiu, 26-28 November 2009, pp. 82-88.

[9] A. Paljanos, S. Miclaus, C. Munteanu, Occupational exposure of personnel operating military radio equipment: measurements and simulation, Electromagnetic Biology and Medicine 34(3) (2015) pp. 221-227. DOI: https://doi.org/10.3109/15368378.2015.1076446

[10] M. J. Hagmann, O. P. Ghandi, C. H. Durney, Numerical calculations of electromagnetic energy deposition for a realistic model of man, IEEE Trans. Microwave Theory Tech. 27(9) (1979) pp. 804-809. DOI: https://doi.org/10.1109/TMTT.1979.1129735

[11] G. I. Rawlandson, P. W. Barbeer, Absorption of higher-frequency RF energy by biological models: Calculations based on geometrical optics, Radio Science 14(6S) (1979) pp. 43-50. DOI: https://doi.org/10.1029/RS014i06Sp00043

[12] H. Massoudi, C. H. Dourney, P. W. Barber, M. F. Iskander, Electromagnetic absorption in multilayered cylindrical models of man, IEEE Trans. Microwave Theory Tech. 27(10) (1979) pp. 825-830. DOI: https://doi.org/10.1109/TMTT.1979.1129742

[13] M. J. Ackerman, The visible human project, Proceedings of the IEEE, 86(3) (1998) pp. 504-511. DOI: https://doi.org/10.1109/5.662875

[14] M. Caon, Voxel-based computational models of real human anatomy: a review, Radiation and Environmental Biophysics 42

(2004) pp. 229–235. DOI: https://doi.org/10.1007/s00411-003-0221-8

[15] ANSYS, https://www.ansys.com

[16] COMSOL MULTIPHYSICS, https://www.comsol.com/

[17] CST STUDIO SUITE, https://www.cst.com/

[18] S. Kuwano, K. Kokubun, Further Study of Microwave Power Absorption in a Multilayered Cylindrical Model of Man, The Journal of Microwave Power and Electromagnetic Energy 32(1) (1997) pp. 45-49. DOI: https://doi.org/10.1080/08327823.1997.11688322

[19] A. Taflove, Advances in Computational Electrodynamics: The Finite-Difference Time-Domain Method, Artech House, Norwood, 1998, ISBN: 0-89006-834-8.

[20] M. Clemens, T. Weiland, Discrete electromagnetism with the finite integration technique, Progress in Electromagnetism Research 32 (2001) pp. 65-87. Online [Accessed 28 September 2020] DOI: https://doi.org/10.2528/PIER00080103

[21] C. M. Furse, J. Y. Chen, O. P. Gandhi, The use of the frequency-dependent finite-difference time-domain method for induced current and SAR calculations for a heterogeneous model of human body, IEEE Trans. on Electromagnetic Compatibility, 36(2) (1994) pp. 128 - 133. DOI: https://doi.org/10.1109/15.293278

[22] O. Bejenaru, C. Lazarescu, S. Vornicu, V. David, Specific Absorption Rate Evaluation in Case of Exposure of the Human Body to Radiofrequency Electromagnetic Field Generated by Mobile Communications, 2018 International Conference and Exposition on Electrical And Power Engineering (EPE), Iasi, Romania, 18 – 19 October 2018. DOI: https://doi.org/10.1109/ICEPE.2018.8559927

[23] A. Laissaoui, B. Nekhoul, K. Kerroum, K. El Khamlichi Drissi, D. Poljak, On the Rotationally-Cylindrical Model of the Human Body Exposed to ELF Electric Field, Progress In Electromagnetics Research M 29 (2013) pp. 165-179. Online [Accessed 28 September 2020] DOI: https://doi.org/10.2528/PIERM13012812

[24] S. Mezoued, B. Nekhoul, D. Poljak, K. El Khamlichi Drissi, K. Kerroum, Human Exposure to transient electromagnetic field using simplified body models, Engineering Analysis with Boundary Elements 34 (2010) pp. 23-29. DOI: https://doi.org/10.1016/j.enganabound.2009.07.013

[25] https://en.wikipedia.org/wiki/Lead_glass

[26] O. Bejenaru, C. Lazarescu, M. Paulet, A. Salceanu, On the convergence of Specific Absorption Rate Values for Human Exposure to Electromagnetic Fields Produced by Mobile Communications Systems, Proc. of 11th International Symposium Advanced Topics in Electrical Engineering, Bucharest, Romania, 28-30 March 2019. DOI: https://doi.org/10.1109/ATEE.2019.8725013

[27] O. Bejenaru, C. Lazarescu, M. Paulet, A. Salceanu, Study upon Specific Absorption Rate: Far Field Source outside and Subject inside the Building, Proc. of 23rd IMEKO TC 4 International Symposium, Xi'an, China, 2019, pp. 176-189. URL: https://www.imeko.org/publications/tc4-2019/IMEKO-TC4-2019-038.pdf

[28] O. Bejenaru, C. Lazarescu., A. Salceanu, V. David, Study Upon Specific Absorption Rate Values for Different Generations of Mobile Phones by Using a SATIMO-COMOSAR Evaluation Dosimetry System, Proc. of the 12th International Conference on Electromechanical and Power Systems (SIELMEN), Chisinau, Republic of Moldova, 9-11 October 2019, pp 355-359. DOI: https://doi.org/10.1109/SIELMEN.2019.8905798